



Dietary versatility of Early Pleistocene hominins

Tina Lüdecke^{a,1}, Ottmar Kullmer^{b,c}, Ulrike Wacker^{d,2}, Oliver Sandrock^e, Jens Fiebig^{a,d}, Friedemann Schrenk^{b,c}, and Andreas Mulch^{a,d}

^aSenckenberg Biodiversity and Climate Research Centre, 60325 Frankfurt, Germany; ^bDepartment of Paleoanthropology, Senckenberg Research Institute and Natural History Museum Frankfurt, 60325 Frankfurt, Germany; ^cInstitute for Ecology, Evolution and Diversity, Department of Paleobiology and Environment, Goethe University, 60439 Frankfurt, Germany; ^dInstitute of Geosciences, Goethe University, 60438 Frankfurt, Germany; and ^eEarth- and Life History, Hessisches Landesmuseum, 64283 Darmstadt, Germany

Edited by Thure E. Cerling, University of Utah, Salt Lake City, UT, and approved November 5, 2018 (received for review June 1, 2018)

New geochemical data from the Malawi Rift (Chiwondo Beds, Karonga Basin) fill a major spatial gap in our knowledge of hominin adaptations on a continental scale. Oxygen ($\delta^{18}\text{O}$), carbon ($\delta^{13}\text{C}$), and clumped (Δ_{47}) isotope data on paleosols, hominins, and selected fauna elucidate an unexpected diversity in the Pleistocene hominin diet in the various habitats of the East African Rift System (EARS). Food sources of early *Homo* and *Paranthropus* thriving in relatively cool and wet wooded savanna ecosystems along the western shore of paleolake Malawi contained a large fraction of C_3 plant material. Complementary water consumption reconstructions suggest that ca. 2.4 Ma, early *Homo* (*Homo rudolfensis*) and *Paranthropus* (*Paranthropus boisei*) remained rather stationary near freshwater sources along the lake margins. Time-equivalent *Paranthropus aethiopicus* from the Eastern Rift further north in the EARS consumed a higher fraction of C_4 resources, an adaptation that grew more pronounced with increasing openness of the savanna setting after 2 Ma, while *Homo* maintained a high versatility. However, southern African *Paranthropus robustus* had, similar to the Malawi Rift individuals, C_3 -dominated feeding strategies throughout the Early Pleistocene. Collectively, the stable isotope and faunal data presented here document that early *Homo* and *Paranthropus* were dietary opportunists and able to cope with a wide range of paleohabitats, which clearly demonstrates their high behavioral flexibility in the African Early Pleistocene.

hominin adaptation | paleoecology | paleodiet | clumped isotopes | Malawi Rift

Dietary adaptations are responsible for significant behavioral and ecological differences among humans and other primates (1, 2). Early hominin diets in Africa before 4 Ma were dominated by C_3 resources and diversified over time (3). Increasing contributions of C_4 plants were triggered by biomes gradually shifting to more open C_4 grasslands since the Late Miocene (4–8). In eastern Africa, dietary versatility was very likely an integral part of early hominin adaptations to open landscapes (7, 9–12), yet it is unclear whether this assumption holds for African Early Pleistocene hominin evolution in general.

Here, we present multiproxy carbon ($\delta^{13}\text{C}$), oxygen ($\delta^{18}\text{O}$), and clumped (Δ_{47}) isotope data focusing on paleoenvironmental patterns and diets of *Paranthropus boisei* and *Homo rudolfensis*. Both hominin taxa coexisted around 2.4 Ma in the Western (Malawi) Branch, the southern part of the East African Rift System (EARS), a region representing a large geographical gap in our knowledge of Early Pleistocene hominin adaptations on a continental scale (13–16). Paleosol development characterizes the lacustrine and deltaic deposits of the Chiwondo Beds (Karonga Basin, northern Malawi) (16). These deposits yielded remains of *H. rudolfensis* at Uraha (17) and Mwenirondo (15), as well as *Paranthropus* remains at Malema, which were assigned to *P. boisei* due to, for example, tooth morphology and palatal height (18). Collectively, these hominin localities of the Chiwondo Beds are less than 50 km apart and are situated today in the Zambesi Ecozone of the African Savannas just south of the boundary to the Somali-Masai Ecozone, and hence outlining the southernmost extent of the Intertropical Convergence Zone. Given this unique location,

the Chiwondo Beds data are crucial for understanding hominin–environment interactions and are broadening our view on habitat flexibility and dietary adaptation in early hominins.

The Karonga Basin lies in the southeastern African hominin corridor region, connecting eastern and southern African endemic faunal zones (19). Hominins thriving in these faunal zones indicate different behaviors: Eastern African *Paranthropus robustus* had a mixed to C_4 -dominated diet around 2.4 Ma, while *P. boisei*, younger than 2 Ma, provides robust evidence for C_4 -dominated consumption in this region. This clearly distinguishes them from age-equivalent southern African *P. robustus*, which shows mixed or C_3 -dominated diets (20–23). Early *Homo* had a highly variable diet, including C_3 and C_4 resources (3, 6).

In contrast to the mostly open C_4 grasslands of the northern EARS, the Malawi Rift was dominantly covered by persistent wooded savannas throughout the Plio-Pleistocene (24). Despite exhibiting a woody cover exceeding 60% and only regional patches of open C_4 grasslands (24, 25), this part of the EARS was populated by early *P. boisei* and *H. rudolfensis*, pointing to a much broader dietary versatility of early East African *P. boisei* than previously assumed.

We utilize a multiproxy approach for reconstructing habitats and diets during the earliest phases of coexisting *Homo* and *Paranthropus* in the Malawi Rift. Our study of $\delta^{13}\text{C}$ and $\delta^{18}\text{O}$ values in tooth enamel of *H. rudolfensis* and *P. boisei* provides insight into dietary preferences, flexibility, and adaptation in variably open and closed savanna environments. In contrast,

Significance

Clumped and stable isotope data of paleosol carbonate and fossil tooth enamel inform about paleoenvironments of Early Pleistocene hominins. Data on woodland- vs. grassland-dominated ecosystems, soil temperatures, aridity, and the diet of *Homo rudolfensis* and *Paranthropus boisei* ca. 2.4 Ma show that they were adapted to C_3 resources in wooded savanna environments in relatively cool and wet climates in the Malawi Rift. In contrast, time-equivalent *Paranthropus* living in open and drier settings in the northern East African Rift relied on C_4 plants, a trend that became enhanced after 2 Ma, while southern African *Paranthropus* persistently relied mainly on C_3 resources. In its early evolutionary history, *Homo* already showed a high versatility, suggesting that Pleistocene *Homo* and *Paranthropus* were already dietary generalists.

Author contributions: T.L., O.K., F.S., and A.M. designed research; T.L. performed research; T.L., U.W., and J.F. contributed new reagents/analytic tools; T.L. analyzed data; and T.L., O.K., O.S., F.S., and A.M. wrote the paper.

The authors declare no conflict of interest.

This article is a PNAS Direct Submission.

This open access article is distributed under [Creative Commons Attribution-NonCommercial-NoDerivatives License 4.0 \(CC BY-NC-ND\)](https://creativecommons.org/licenses/by-nc-nd/4.0/).

¹To whom correspondence should be addressed. Email: tina.luedecke@senckenberg.de.

²Present address: Thermo Scientific GmbH, 28199 Bremen, Germany.

This article contains supporting information online at www.pnas.org/lookup/suppl/doi:10.1073/pnas.1809439115/-DCSupplemental.

Published online December 10, 2018.

intratooth $\delta^{13}\text{C}$ and $\delta^{18}\text{O}$ time series from contemporaneous equids (*Eurygnathohippus* sp.) and bovids [Alcelaphinae (Alc.) *Megalotragus* sp.], in addition to $\delta^{13}\text{C}$ and $\delta^{18}\text{O}$ data from pedogenic carbonate of the hominin fossil sites, allow the reconstruction of vegetation patterns (25, 26). The Δ_{47} data from paleosols of the hominin fossil sites are from the southern part of the EARS and provide insight into regional temperature differences during the time of early hominin evolution. Our results show that early hominins must have been able to adapt to different environmental settings and diets as early as 2.4 Ma, indicating high behavioral flexibility already in the early stages of hominin evolution, as first indicated by, for example, Turkana Basin *Kenyanthropus platyops* individuals at 3.4–3.0 Ma (3).

Results

We report $\delta^{13}\text{C}$ and $\delta^{18}\text{O}$ data from tooth enamel of all three Chiwondo Bed hominin individuals, as well as age-equivalent bovid ($n = 2$) and equid ($n = 3$) specimens [sample IDs stated according to the Hominin Corridor Research Project (HCRP), with location ID followed by the individual sample number]. We complement these by $\delta^{13}\text{C}$ and $\delta^{18}\text{O}$ ($n = 199$ samples) as well as Δ_{47} thermometry ($n = 12$ samples) data of pedogenic carbonate. All samples originate from unit 3-A2 (ca. 2.5–2.3 Ma) of the Chiwondo Beds (27) in the Karonga Basin at the northwest margin of Lake Malawi. In addition, we present modern soil temperatures that were monitored at three locations (full shade, partial shade, and full sun) throughout a complete year ($n = 26,280$ measurements) in the depth of typical pedogenic carbonate precipitation within the region (~40 cm below the surface). Results are shown in Figs. 1–3 and listed in *SI Appendix, Tables S2–S8*.

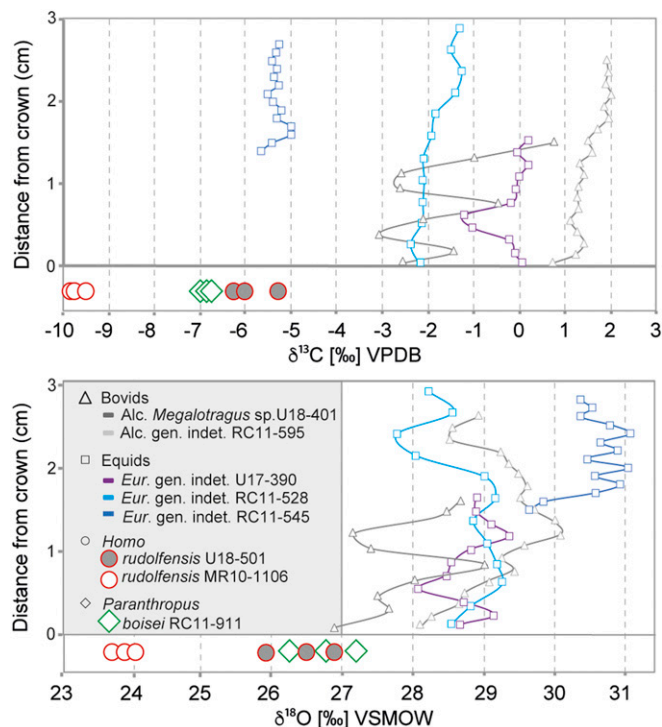


Fig. 1. Intratooth $\delta^{13}\text{C}$ and $\delta^{18}\text{O}$ variations in equid and bovid teeth vs. distance from the crown; hence, time of tooth growth. The hominin tooth enamel sample quantity was too small to determine intratooth patterns; each sample averages almost the entire interval of enamel development. Bovid and equid were coexistent with the early hominins, and fossils were collected at the same localities. Different patterns indicate different migratory behavior of the individuals and/or seasonal changes. Eur., *Eurygnathohippus*; gen. indet., genus indeterminate.

Hominin and Herbivore Tooth Enamel $\delta^{13}\text{C}$ and $\delta^{18}\text{O}$ Data.

H. rudolfensis. Each tooth shows only a small range in $\delta^{13}\text{C}$ and $\delta^{18}\text{O}$ values, but the two individuals show a clear geochemical distinction in their tooth enamel, with a mean difference of 3.8‰ in $\delta^{13}\text{C}$ and 2.5‰ in $\delta^{18}\text{O}$ (Fig. 1).

The $\delta^{13}\text{C}$ and $\delta^{18}\text{O}$ values from the Uraha individual HCRP-U18-501 ($n = 3$) are -6.3‰ , -6.0‰ , and -5.3‰ (mean = -5.9‰ , $\sigma = 0.5\text{‰}$, C_3/C_4 ratio = $\sim 65:35$) and 25.9‰, 26.5‰, and 26.9‰ (mean = 26.4‰, $\sigma = 0.5\text{‰}$), respectively.

The $\delta^{13}\text{C}$ and $\delta^{18}\text{O}$ values from the Mweniirondo specimen HCRP-MR10-1106 ($n = 3$) are more negative, with $\delta^{13}\text{C}$ values of -9.9‰ , -9.8‰ , and -9.5‰ (mean = -9.7‰ , $\sigma = 0.2\text{‰}$, C_3/C_4 ratio = $\sim 95:5$) and $\delta^{18}\text{O}$ values of 23.6‰, 23.9‰, and 24.1‰ (mean = 23.9‰, $\sigma = 0.2\text{‰}$).

P. boisei. The molar from the Malema individual HCRP-RC11-911 ($n = 3$) shows $\delta^{13}\text{C}$ values of -7.0‰ , -6.9‰ , and -6.8‰ (mean = -6.9‰ , $\sigma = 0.1\text{‰}$, C_3/C_4 ratio = $\sim 70:30$). The $\delta^{18}\text{O}$ values are 26.3‰, 26.8‰, and 27.2‰ (mean = 26.8‰, $\sigma = 0.5\text{‰}$).

Bovids (Alcelaphinae). The Alcelaphini *Megalotragus* sp. molar HCRP-U18-401 ($n = 9$) from the *H. rudolfensis* fossil site has much more positive $\delta^{13}\text{C}$ values compared with the hominins, with a range between -2.6‰ and 0.8‰ (mean = -1.7‰ , $\sigma = 1.3\text{‰}$, C_3/C_4 ratio = $\sim 30:70$). The $\delta^{18}\text{O}$ values range between 26.3‰ and 28.4‰ (mean = 27.3‰, $\sigma = 0.7\text{‰}$).

The $\delta^{13}\text{C}$ and $\delta^{18}\text{O}$ values of Alc. genus and sp. indeterminate HCRP-RC11-595 ($n = 19$) from the *P. boisei* locality at Malema are generally even more positive than the *Megalotragus* sp. data; $\delta^{13}\text{C}$ values range from 0.7 to 2.0‰ (mean = 1.5‰, $\sigma = 0.4\text{‰}$, C_3/C_4 ratio = $\sim 2:98$). Only a slight positive shift of 1.3‰ is present in this very narrow range. The $\delta^{18}\text{O}$ values show a curved pattern between 27.5‰ and 29.5‰ (mean = 28.5‰, $\sigma = 0.5\text{‰}$).

Equids (*Eurygnathohippus* sp.). Similar to Alcelaphinae, a very narrow range in $\delta^{13}\text{C}$ values and a larger variability in $\delta^{18}\text{O}$ values characterize the stable isotope data of the three sampled *Eurygnathohippus* sp. teeth from different individuals, which show a clear geochemical distinction, especially in $\delta^{13}\text{C}$ (Fig. 1).

The premolar of HCRP-U17-390 ($n = 11$) (location U17 is the same age and spatially correlated with *H. rudolfensis* from U18) has $\delta^{13}\text{C}$ values between -1.2‰ and 0.2‰ (mean = -0.2‰ , $\sigma = 0.5\text{‰}$, C_3/C_4 ratio = $\sim 15:85$). The $\delta^{18}\text{O}$ values are between 27.5‰ and 28.7‰ (mean = 28.1‰, $\sigma = 0.3$). HCRP-RC11-528 ($n = 12$) from the *P. boisei* site has $\delta^{13}\text{C}$ values between -2.4‰ and -1.3‰ (mean = -1.9‰ , $\sigma = 0.4\text{‰}$, C_3/C_4 ratio = $\sim 30:70$) and $\delta^{18}\text{O}$ values from 27.2 to 28.6‰ (mean = 28.1‰, $\sigma = 0.5\text{‰}$). HCRP-RC11-545 ($n = 14$) also shows more negative $\delta^{13}\text{C}$ values than the other *Eurygnathohippus* sp., with a very narrow range from -5.7 to -5.0‰ (mean = -5.3‰ , $\sigma = 0.2\text{‰}$, C_3/C_4 ratio = $\sim 50:50$), while the $\delta^{18}\text{O}$ values are generally more positive, between 29.0‰ and 30.3‰ (mean = 29.8‰, $\sigma = 0.4\text{‰}$).

Pedogenic Carbonate Δ_{47} Temperatures. Pedogenic carbonate Δ_{47} temperatures from the *H. rudolfensis* site U18 (Uraha) range from 19 to 38 °C (mean = 28 °C, $\sigma = 8.3$ °C; $n = 6$). The dataset seems to be bimodal, with values grouping at relatively high temperatures (mean = 35 °C, $\sigma = 2.2$ °C; $n = 3$) and another cluster of low temperatures (mean = 21 °C, $\sigma = 1.8$ °C; $n = 3$). A trend over time (i.e., across the sampled fossil horizon) is not present.

Paleosol temperatures from the *P. boisei* site RC11 (Malema) show a smaller variation, with values between 22 °C and 29 °C (mean = 26 °C, $\sigma = 2.9$ °C; $n = 6$).

Karonga Basin soil water $\delta^{18}\text{O}$ values ($\delta^{18}\text{O}_{\text{SW}}$) were calculated using the $\delta^{18}\text{O}$ values of the carbonate and their Δ_{47} temperatures according to the methods of Kim et al. (28) and Kim and O'Neil (29), resulting in $\delta^{18}\text{O}_{\text{SW}}$ values between -5.4‰ and -1.5‰ (mean = 3.6‰, $\sigma = 1.2\text{‰}$ °C; $n = 12$).

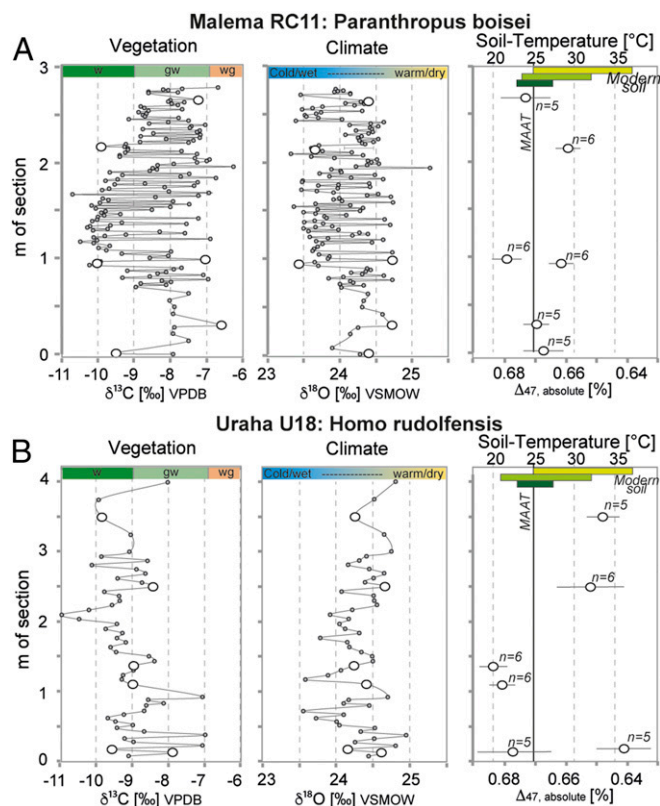


Fig. 2. $\delta^{13}\text{C}$, $\delta^{18}\text{O}$, and Δ_{47} values for Karonga Basin paleosol carbonate from the 2.5- to 2.3-Ma-old hominin fossil sites of Malema (A) and Uraha (B). Definitions of biome abbreviations are provided in Fig. 4. The black line shows modern MAAT.

Pedogenic Carbonate $\delta^{13}\text{C}$ and $\delta^{18}\text{O}$ Values.

Uraha. The $\delta^{13}\text{C}$ values of pedogenic carbonate from a soil profile at the *H. rudolfensis* site U18 ($n = 52$) range between -11.0‰ and -7.0‰ (mean = -9.1‰ , $\sigma = 0.8\text{‰}$). The estimated fraction of woody cover (f_{wc}) (5) ranges between 0.5 and 0.8. The corresponding $\delta^{18}\text{O}$ values lie between 23.6‰ and 24.9‰ (mean = 24.3‰ , $\sigma = 0.3\text{‰}$).

Malema. The $\delta^{13}\text{C}$ values of pedogenic carbonate from the *P. boisei* site RC11 ($n = 147$) cover a similar range as at the Uraha site, with $\delta^{13}\text{C}$ values between -10.7‰ and -6.3‰ (mean = 8.5‰ , $\sigma = 1.1\text{‰}$). The estimated f_{wc} values range from 0.4 to 0.8. The $\delta^{18}\text{O}$ values show a slightly larger variation than at the Uraha site, with values between 23.3‰ and 24.7‰ , excluding one outlier with a value of 25.2‰ (mean = 24.1‰ , $\sigma = 0.4\text{‰}$).

Correlation Between Stable and Clumped Isotope Data. (Negative) correlation between datasets was determined by using the Pearson correlation coefficient. Statistically (negative) correlation is significant at the 95% level.

We observe a statistically relevant positive correlation between $\delta^{18}\text{O}$ and $\delta^{13}\text{C}$ values in the Uraha ($P = 0.5$) and Malema ($P = 0.8$) datasets, suggesting a higher fraction of woody cover during periods of wetter climates.

Reconstructed Δ_{47} soil temperatures and $\delta^{18}\text{O}$ and $\delta^{13}\text{C}$ values show a strong negative correlation at the Malema site RC11 ($P = -0.9$ for $\delta^{18}\text{O}$ and $P = -0.8$ for $\delta^{13}\text{C}$); hence, high (soil) temperatures coincide with a moister climate, which produces an even denser canopy cover serving as a buffer and resulting in less thermal loss at night. This is complemented by the small range in soil temperatures at this site (Fig. 5).

Modern Soil Temperatures. Soil temperatures were measured hourly 40 cm below the surface under conditions of full shade, partial shade, and full sun (Fig. 3).

Full shade. Over the course of 1 y (August 1, 2016 to July 31, 2017), soil temperatures in sandy soil under dense tree cover range from ca. 23 to 27 °C (mean = 26 °C, $\sigma = 0.9$ °C; $n = 8,760$). Temperature differences between day and night, as well as between dry and wet seasons, are relatively small (generally ca. 0.5 °C and 2 °C, respectively).

Partial shade. Recorded soil temperatures (August 1, 2016 to July 31, 2017) show a range of 21 to 32 °C (mean = 27 °C, $\sigma = 2.1$ °C; $n = 8,760$) ~50 m away from the full-shade location. Here, temperatures below 24 °C are limited to a few outliers ($n = 98$; i.e., 1%) during the wet season, probably due to extreme rainfall and resulting soil water saturation. Day/night differences at around 0.5 °C are comparable to the full-shade site, but the difference between dry and wet seasons is more pronounced, with almost 6 °C warmer soil temperatures during the end of the dry season.

Full sun. Soil temperature loggers were put directly in the Chiwondo Bed sandy deltaic deposits at the open habitat of the Malema *P. boisei* site (RC11). The recorded temperatures (August 15, 2016 to August 14, 2017) are higher than at the locations of full shade and partial shade and range from 25 to 37 °C (mean = 31 °C, $\sigma = 3.2$ °C; $n = 8,760$). Day/night temperature differences are >2 °C and increase during the rainy season, with maximum day temperatures of generally 36 °C contrasting with night temperatures, which regularly drop below 32 °C.

Discussion

Paleoenvironmental Reconstruction of *H. rudolfensis* and *P. boisei* Sites in the Karonga Basin.

The results of paleosol stable isotope geochemistry from the Karonga Basin hominin sites indicate woodland, bushland, and scrubland to grassy woodland environments characterized by 40–80% woody cover (Figs. 3 and 4 and *SI Appendix, Tables S4 and S5*) during the time of early hominin occupation at ca. 2.5–2.3 Ma. Reconstructed mean paleosol Δ_{47} temperatures attain 26 °C for the Malema *P. boisei* (Malema) site and 28 °C at the Uraha *H. rudolfensis* (Uraha) site, which are similar to today's partial shade soil temperatures in the region (Figs. 3 and 5). Especially the Malema Δ_{47} temperatures (usually reflecting soil temperatures below 30 cm), which are considered to have a strong seasonal bias toward dry and warm periods when carbonate precipitation predominantly occurs, are relatively cool compared with the Eastern Rift paleosol temperature data of 2.8–1.8 Ma, which are typically in excess of 35 °C (30) (e.g., Turkana; Fig. 5), indicating that hominins

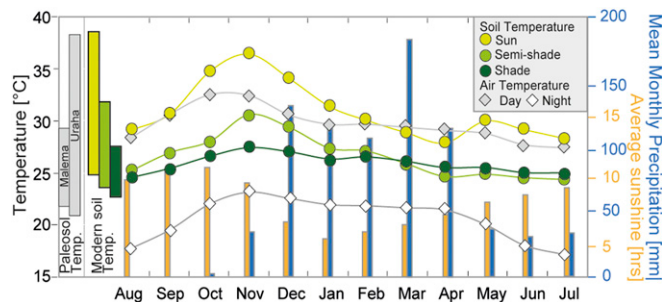


Fig. 3. Mean monthly soil temperatures (circles) measured for this study (2016/2017) with day and night air temperatures (diamonds), mean precipitation (blue), and average sunshine hours (orange) (32). Soil temperatures (columns on the left represent the complete temperature span of the full year in the respective color) generally follow air temperature patterns and correlate with sunshine hours, especially in soil directly exposed to the sun; here, the soil is usually warmer than the air due to the effect of direct solar radiation. Bars at the left of the figure show the maximum range of measured soil temperatures at the different locations. Temp., temperature.

thrived under different temperature conditions in different parts of the EARS during the Early Pleistocene.

The present-day Karonga Basin is characterized by a tropical savanna climate (31) with mean annual air temperatures (MAATs) of $\sim 25^\circ\text{C}$ and mean annual precipitation (MAP) of $\sim 1,170\text{ mm}\cdot\text{y}^{-1}$ (32), which results in the wooded savanna ecosystem of the Zambezi woodland savanna. The Turkana Basin, in contrast, is characterized by a hot desert/semiarid climate (31), with MAATs exceeding 29°C and MAP $< 200\text{ mm}$ (32), creating open savanna settings with dominantly C_4 grasses, similar to reconstructed landscapes in the Early Pleistocene (Fig. 4). Soils exposed to direct sunlight at both localities exhibit soil temperatures ($>35^\circ\text{C}$) that are typically warmer than measured air temperatures (5, 30) (Figs. 3 and 5), reflecting the effect of radiative heating under sparse canopy cover. This indicates that the generally lower Karonga soil temperatures during the Early Pleistocene were triggered, among other factors, by a higher fraction of woody cover in the southern part of the EARS. Complementary calculated Karonga Basin $\delta^{18}\text{O}_{\text{soilwater}}$ data (depending on $\delta^{18}\text{O}$ values of the carbonate and their Δ_{47} temperature) show *ca.* 5‰ more negative average values than the Turkana data (30), pointing to a smaller effect of evaporation of the soil water in the southern part of the EARS. The $\delta^{18}\text{O}$ values from Karonga Basin pedogenic carbonates are generally lower than data observed at most other African hominin sites (ref. 33 and references therein), which suggests more humid conditions and less influence of evaporation in the cooler and more wooded habitats of the Malawi Rift in contrast to those of eastern Africa.

Consequently, larger fractions of woody cover imply more shade, shelter, and dietary resources for early hominins in the Zambesi Ecozone in the Malawi Rift, accompanied by lower air temperatures during the dry season. Ecosystem diversity of the Pleistocene Karonga Basin is reflected by the high ($<30^\circ\text{C}$) reconstructed soil temperatures of individual pedogenic carbonates from the Uraha site, pointing to temporary direct sun exposure of the soil in a possibly patchy landscape (also ref. 25).

Intratooth $\delta^{13}\text{C}$ variability (-5.7 to 2.0‰) of herbivorous mammals coexisting with *H. rudolfensis* and *P. boisei* indicate that both C_3 and C_4 vegetation was available for consumption, which permitted highly variable foraging strategies for migrating mammals (25). Alcelaphini and equids were able to either feed almost selectively on C_4 resources or exhibit mixed grazing and browsing foraging strategies (25) (Fig. 1). These migrating and often specialized feeders, however, do not necessarily reflect the dominant paleoenvironment, but typically select their dietary niche. On the contrary, (Pleistocene) suids are considered generalists, and suid enamel $\delta^{13}\text{C}$ values hence average local resource $\delta^{13}\text{C}$ variability. The $\delta^{13}\text{C}$ tooth enamel data for Karonga Basin Plio-Pleistocene suids indicate a predominantly C_3 browsing diet during the time of early *Homo* sp. evolution (24) (Fig. 6). This suggests that early Karonga Basin hominins had

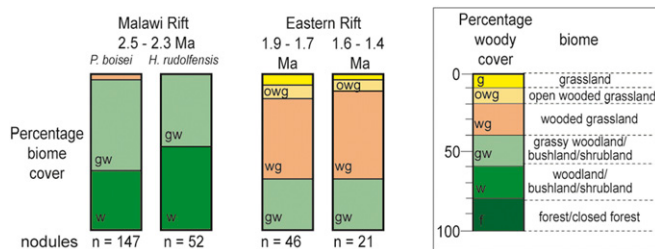


Fig. 4. Comparison of environmental proxies between the Malawi Rift and Eastern Rift. Biome cover, relative proportions of biomes based on paleosol $\delta^{13}\text{C}$ values (5), and boundaries between biomes are described in *SI Appendix*. The Malawi Rift was dominated by a more wooded environment (in a generally moister and cooler climate; Fig. 5) during the time of early hominin evolution compared with the Eastern Rift.

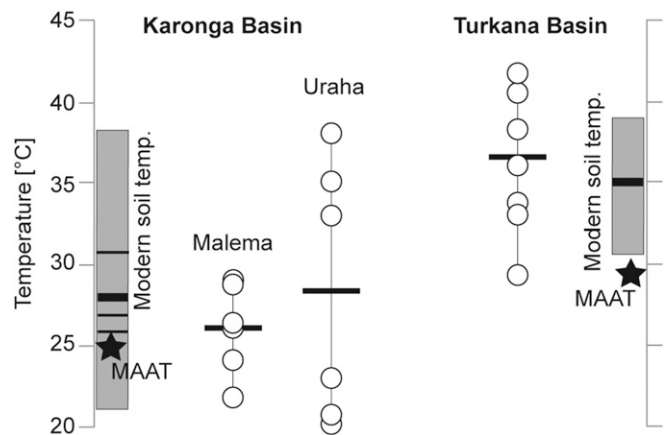


Fig. 5. Clumped isotope paleosol temperatures (\circ , with black lines representing the mean) from paleosol carbonates of the Karonga Basin ($n = 12$) vs. the Turkana Basin ($n = 8$) (30) between 2.8 Ma and 1.8 Ma. For direct comparison, the Turkana Basin Δ_{47} data were recalculated to the absolute reference frame using the technique of Uno et al. (49) and the calibration of Cerling et al. (50) (*SI Appendix, Table S1*). Gray bars represent today's minimum to maximum soil temperatures in 40 cm (Karonga Basin) or 50 cm (Turkana Basin), with the thick line as the overall mean. Turkana Basin soil temperatures are measured under sparse deciduous bush vegetation, while the thin lines in the Karonga Basin data represent mean temperatures of soils exposed to full sun (top), partial shade (middle), and full shade (bottom). Black stars show MAATs. Similar to modern data, reconstructed soil temperatures are generally lower in the Karonga Basin, which created a landscape with different (food) resources than in the hotter Turkana Basin. Temp., temperature.

access to a wide range of vegetation types, such as gallery forest near the freshwater sources and open C_4 grasslands in the more elevated or arid regions at the rift shoulders, providing a diverse spectrum in food supply and shelter (cf. refs. 24, 25).

Diets of Early *H. rudolfensis* and *P. boisei* in the Malawi Rift. The $\delta^{13}\text{C}$ values of the Karonga Basin hominins at *ca.* 2.4 Ma suggest variable, mixed diets with only small portions of C_4 intake ($<40\%$; Fig. 6). Stable isotope geochemical data suggest that the two *H. rudolfensis* individuals showed different foraging strategies. HCRP-U18-501 was a mixed feeder with 60–70% C_3 resources, while HCRP-MR10-1106 fed almost exclusively on C_3 resources and had less than 6% C_4 intake (Fig. 6). This suggests an adaptation to versatile ecosystem parameters with varying types of food supply and/or selective foraging strategies. The coexisting *P. boisei* individual reflects a similar diet, where C_3 resources amounted to *ca.* 70%. Early *Paranthropus* in the Karonga Basin therefore relied heavily on the presence of woodland habitats.

The two analyzed hominin taxa are geochemically indistinguishable due to the relatively large spread in $\delta^{13}\text{C}$ and $\delta^{18}\text{O}$ values measured for the two individuals of *H. rudolfensis* and the fact that *P. boisei* isotope data lie within the same range (Figs. 1 and 6).

The $\delta^{13}\text{C}$ values of *Homo* and *Paranthropus* point to food intake that consisted dominantly of C_3 resources, such as forest foods, while xeric plant foods [e.g., C_4 underground storage organs (USOs), such as tubers, corms, roots, and bulbs, but also sedges, termites (20, 34, 35), or C_4 grass leaves (36)] were not dominant. However, $\delta^{13}\text{C}$ data alone may not decipher C_3 and C_4 resources of dietary patterns because plant-based, meat-based, and omnivore diets cannot be distinguished with this method (e.g., ref. 37).

The narrow range of soil water and paleosol carbonate $\delta^{18}\text{O}$ values from the Karonga Basin hominin sites (Fig. 2) suggests relatively constant climatic conditions in the vicinity of paleolake Malawi. *H. rudolfensis* individual HCRP-MR-1106 shows the lowest $\delta^{18}\text{O}$ values, while the $\delta^{18}\text{O}$ values of *H. rudolfensis* HCRP-UR-501 and *P. boisei* HCRP-RC-911 overlap. The

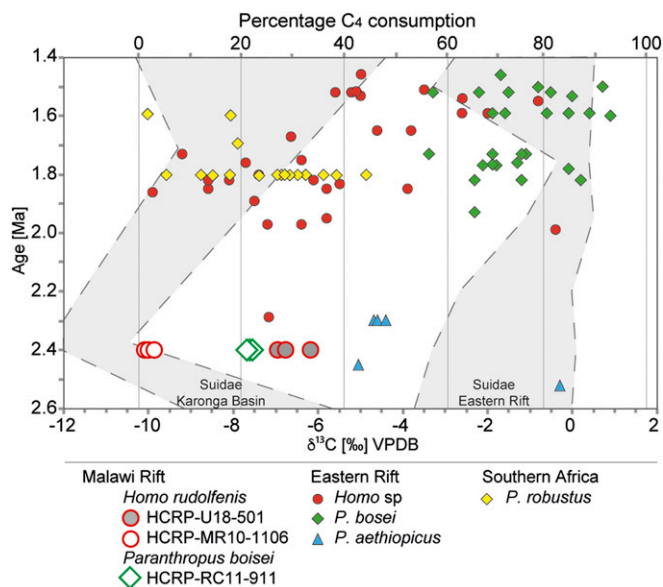


Fig. 6. $\delta^{13}\text{C}$ values of hominin tooth enamel with respect to the age of the fossils. Karonga Basin Malawi *H. rudolfensis* and *P. boisei* of this study are compared with *Homo* sp., *P. boisei*, and *P. aethiopicus* of the Turkana Basin (3) and *P. robustus* from South Africa (20–23). The percentage of C_4 consumption is calculated using the method of Cerling et al. (5) and is explained in *SI Appendix*. Especially *P. boisei* of the Karonga Basin therefore had a diet much more influenced by C_3 intake than their younger Eastern Rift relatives, indicating an adaptation to more open environments in the Eastern Rift. Gray areas indicate $\delta^{13}\text{C}$ values of coexisting suids for the Karonga Basin (16) (Left) and the Eastern Rift (49–56) (Right), reflecting a dominantly C_3 diet of Karonga Basin omnivores and a highly C_4 -influenced diet of Eastern Rift ones, which, in turn, reflects the main vegetation type of the hominin sites.

relatively low $\delta^{18}\text{O}$ values in concert with the $\delta^{13}\text{C}$ data render it likely that both hominin taxa had access to drinking water only little affected by evaporation (and associated ^{18}O -enrichment). The $\delta^{18}\text{O}$ values of the hominin teeth are generally lower than the $\delta^{18}\text{O}$ values from coexisting bovids and equids (Fig. 1). The spread in $\delta^{18}\text{O}$ values of tooth enamel of both *Megalotragus* sp. and *Eurygnathohippus* sp. is larger than the scatter measured for the hominin individuals. Migrating herbivores had access to different drinking water sources of distinct oxygen isotope compositions, whereas hominins probably remained rather stationary near freshwater sources, such as tributaries of paleolake Malawi.

Comparison with Other African Hominins. Stable carbon isotope analysis of African hominins suggests an increasing intake of C_4 biomass between ca. 4.1 Ma and 1.4 Ma throughout eastern, southern, and central Africa (Fig. 6). While hominins prior to 4 Ma (e.g., *Ardipithecus ramidus* and *Australopithecus anamensis*) depended almost fully on C_3 resources, an expansion toward mixed diets that included C_4 resources is observed starting at 3.75 Ma [e.g., *Australopithecus bahrelghazali*, *Australopithecus afarensis*, *K. platyops*, Hominini indet (3, 4, 7, 20, 38–42)]. By ca. 2 Ma, the genus *Homo* had a highly variable mixed C_3/C_4 diet in the Turkana Basin, while *P. boisei* was characterized by a strongly C_4 -dominated diet with only <25% C_3 intake (Fig. 6), pointing to a diet characterized by USOs and other C_4 resources. The evolution of (open) wooded C_4 grassland savannas in the Eastern Rift presents a very different ecological setting from the persistent wooded savanna environments of the Karonga Basin (24, 25) (Fig. 4). This indicates different feeding strategies of *Homo* sp. and *Paranthropus* sp. in the increasingly open grassland savannas of the Eastern Rift (3, 6), and is a potential key for understanding the dietary evolution of early hominins. *H. rudolfensis* HCRP-U18-501 had a similar

diet as younger (ca. 2.3–1.4 Ma) *Homo* species from the Turkana Basin (3). The almost exclusive C_3 diet of individual HCRP-MR10-1106, however, is rarely observed in Pleistocene Turkana hominins; the widely variable diet of eastern African *Homo* sp. rarely includes such selected feeders (3) (Fig. 6), indicating an adjustment to the denser wooded landscape of the Malawi Rift and/or to the more open savanna landscapes in the Eastern Rift.

Based on the existing spatial and temporal coverage of *P. boisei* remains, *P. boisei* adopted a significantly different diet in the diverging biomes of the Eastern Rift and Malawi Rift, supporting an unexpected versatile adaptive behavior. This predicts significantly different feeding strategies of *P. boisei* in the Karonga Basin at ca. 2.4 Ma compared with Turkana Basin individuals dated <2 Ma, which consumed predominantly C_4 biomass (>40%) (6). The latter most likely relied heavily on the intake of sedges (37, 43). In contrast, the Karonga Basin *P. boisei* foraging strategies even involved a higher fraction of C_3 food resources than coexisting Turkana Basin *Paranthropus aethiopicus*, which, in turn, consumed less C_4 plants than the younger *P. boisei* in the same region (3, 6). South African *P. robustus* (Sterkfontein Valley and Gauteng; ca. 1.8–1.0 Ma) probably also lived in a woodland environment and had a similarly mixed diet like *P. boisei* in the Karonga Basin (3, 20–23).

Collectively, this points to an adaptive behavior toward increasing C_4 biomass consumption [e.g., sedges, termites (20, 37) if these were easily accessible] but an enduring C_3 -dominated diet in wooded settings throughout the time of early hominin evolution. However, due to the lack of Karonga Basin hominins younger than 2 Ma and/or sufficient data of Eastern Rift hominins older than 2 Ma that thrived in a woodland-dominated ecosystem, it is difficult to determine if the adaptation could be a supraregional effect or the result of local ecosystem pressure.

Conclusions

Stable carbon and oxygen isotope data of hominin fossil tooth enamel from the Malawi Rift show that early (ca. 2.4 Ma) *H. rudolfensis* and *P. boisei* included a large fraction of C_3 food resources in their diets. Abundant C_3 resources were provided by relatively cool and well-watered wooded savanna ecosystems in the vicinity of paleolake Malawi in the southern part of the EARS. Younger (<2 Ma) *Paranthropus* individuals from the Eastern Rift incorporated an increasing amount of C_4 resources in hotter, more arid, and open savanna settings, while *P. robustus* maintained a C_3 -dominated diet in the wetter and more mesic environments of southern Africa. Throughout the Early Pleistocene, *Homo* shows a high versatility in the diverse habitats of the EARS. *H. rudolfensis* and *P. boisei* were therefore dietary generalists, able to adapt to different paleohabitats, successfully utilizing a broad range of ecosystems, including freshwater environments near the tributaries to paleolake Malawi.

Methods

Teeth of three hominins, three equids, and two bovids temporarily housed in the Senckenberg Research Institute and from the Cultural and Museum Centre Karonga were sampled using a high-speed, rotary, diamond-tip drill to obtain 2.5–5 mg of enamel powder from each of the up to 19 samples per tooth. To remove organic and potential diagenetic carbonate, enamel was pretreated with 2% sodium hypochlorite solution for 24 h, followed by treatment with 1 M Ca-acetate acetic buffer solution for another 24 h (44). Additionally, 199 pedogenic carbonate nodules were analyzed. Then, 600–1,200 μg of pretreated enamel and 100–160 μg of untreated pedogenic carbonate material were reacted with 99% H_3PO_4 for 90 min at 70 °C in continuous flow mode using a Thermo Finnigan 253 mass spectrometer interfaced to a Thermo GasBench II. All analyses were performed at the Goethe University Frankfurt–Senckenberg Biodiversity and Climate Research Centre Stable Isotope Facility. Analytical procedures followed the technique of Spötl and Vennemann (44). Final isotopic ratios are reported versus VPDB (Vienna Pee Dee Belemnite; $\delta^{13}\text{C}$) and VSMOW (Vienna Standard Mean Ocean Water; $\delta^{18}\text{O}$); overall analytical uncertainties are better than 0.3‰.

Homogenized powder of 12 selected soil nodules measured for stable isotopes was additionally used for clumped isotope analyses, which were performed in the same laboratory. Untreated carbonate powder (5–15 mg) was

digested in $\geq 106\%$ H_3PO_4 at $90^\circ C$ for 15–30 min, using a semiautomated acid bath (45, 46). The produced CO_2 was cleaned by flowing through cryogenic traps at $-80^\circ C$ before and after passage through a Porapak Q-packed gas chromatography column to remove traces of water and hydrocarbons (cf. refs. 45, 46). The purified CO_2 was analyzed using a Thermo Scientific MAT 253 gas source isotope ratio mass spectrometer dedicated to the determination of masses 44–49 in 10 acquisitions consisting of 10 cycles each, with an ion integration time of 20 s per cycle. Five to six replicates were run per carbonate sample. The best precision that can be achieved under these conditions is represented by the shot noise limit, which is 0.004% for $n = 5$ and 0.003% for $n = 6$. The Δ_{47} values are reported in the absolute reference frame (47) and were processed according to the protocol of Fiebig et al. (48). Apparent carbonate crystallization temperatures were computed from measured Δ_{47} values using the empirical calibration technique of Wacker et al. (46).

Soil temperatures (quoted accuracy of $\pm 0.1^\circ C$) were measured hourly using Voltcraft DL-101T USB-Temperature loggers, which were buried within polyethylene-plastic bottles ca. 40 cm below the surface in narrow trenches

(~ 15 cm wide), which were subsequently backfilled with the soil removed during excavation.

SI Appendix, Materials and Methods includes additional information on analytical procedures, data processing, dating, time interval recorded in enamel and pedogenic carbonate, isotope enrichment factors in mammals, stratigraphic information, and biome classifications used in this work.

ACKNOWLEDGMENTS. We thank the Cultural Museum Centre Karonga, our local Malawian field crew, and the Malawian Government for the long-term cooperation with the HCRP. We particularly thank H. Simfukwe (Cultural Museum Centre Karonga) for assistance and hospitality. T.L. thanks U. Treffert, N. Löffler, K. Methner (Senckenberg Biodiversity and Climate Research Centre), and S. Hofmann (Goethe University Frankfurt) for laboratory support and H. Thiemeyer (Goethe University Frankfurt) for support in the field. The paper was greatly improved by the thoughtful comments of two anonymous reviewers. T.L. acknowledges funding by Deutsche Forschungsgemeinschaft Grant LU 2199/1-1.

- Ungar P (1998) Dental allometry, morphology, and wear as evidence for diet in fossil primates. *Evol Anthropol* 6:205–217.
- Fleagle J (2013) *Primate Adaptation and Evolution* (Academic, San Diego), 3rd Ed.
- Cerling TE, et al. (2013) Stable isotope-based diet reconstructions of Turkana Basin hominins. *Proc Natl Acad Sci USA* 110:10501–10506.
- Sponheimer M, et al. (2013) Isotopic evidence of early hominin diets. *Proc Natl Acad Sci USA* 110:10513–10518.
- Cerling TE, et al. (2011) Woody cover and hominin environments in the past 6 million years. *Nature* 476:51–56.
- Cerling TE, et al. (2011) Diet of *Paranthropus boisei* in the early Pleistocene of East Africa. *Proc Natl Acad Sci USA* 108:9337–9341.
- Levin NE, Haile-Selassie Y, Frost SR, Saylor BZ (2015) Dietary change among hominins and cercopithecids in Ethiopia during the early Pliocene. *Proc Natl Acad Sci USA* 112:12304–12309.
- Uno KT, et al. (2018) Large mammal diets and paleoecology across the Oldowan-Acheulean transition at Olduvai Gorge, Tanzania from stable isotope and tooth wear analyses. *J Hum Evol* 120:76–91.
- Ungar PS, Grine FE, Teaford MF (2006) Diet in early Homo: A review of the evidence and a new model of adaptive versatility. *Annu Rev Anthropol* 35:209–228.
- Teaford MF, Ungar PS (2000) Diet and the evolution of the earliest human ancestors. *Proc Natl Acad Sci USA* 97:13506–13511.
- Ungar PS, Grine FE, Teaford MF (2008) Dental microwear and diet of the Plio-Pleistocene hominin *Paranthropus boisei*. *PLoS One* 3:e2044.
- Scott RS, et al. (2005) Dental microwear texture analysis shows within-species diet variability in fossil hominins. *Nature* 436:693–695.
- Bromage TG, Schrenk F, Zonneveld FW (1995) Paleoanthropology of the Malawi rift: An early hominid mandible from the Chiwondo Beds, northern Malawi. *J Hum Evol* 28:71–108.
- Schrenk F, Kullmer O, Sandrock O, Bromage TG (2002) Early hominid diversity, age and biogeography of the Malawi-rift. *J Hum Evol* 17:113–122.
- Kullmer O, et al. (2011) New primate remains from Mwenirondo, Chiwondo Beds in northern Malawi. *J Hum Evol* 61:617–623.
- Lüdecke T, Thiemeyer H (2013) Paleoenvironmental characteristics of the Plio-Pleistocene Chiwondo and Chitimwe Beds (N-Malawi). *J Palaeoecol Afr* 32:143–161.
- Schrenk F, Bromage TG, Betzler CG, Ring U, Juwayeyi YM (1993) Oldest *Homo* and Pliocene biogeography of the Malawi rift. *Nature* 365:833–836.
- Kullmer O, et al. (1999) The first *Paranthropus* from the Malawi rift. *J Hum Evol* 37:121–127.
- Bromage TG, Schrenk F (1995) Biogeographic and climatic basis for a narrative of early hominid evolution. *J Hum Evol* 28:109–114.
- Sponheimer M, et al. (2005) Hominins, sedges, and termites: New carbon isotope data from the Sterkfontein valley and Kruger National Park. *J Hum Evol* 48:301–312.
- Sponheimer M, et al. (2006) Isotopic evidence for dietary variability in the early hominin *Paranthropus robustus*. *Science* 314:980–982.
- Lee-Thorp J, Thackeray JF, van der Merwe N (2000) The hunters and the hunted revisited. *J Hum Evol* 39:565–576.
- Lee-Thorp JA, van der Merwe NJ, Brain CK (1994) Diet of *Australopithecus robustus* at Swartkrans from stable carbon isotopic analysis. *J Hum Evol* 27:361–372.
- Lüdecke T, et al. (2016) Persistent C_3 vegetation accompanied Plio-Pleistocene hominin evolution in the Malawi rift (Chiwondo Beds, Malawi). *J Hum Evol* 90:163–175.
- Lüdecke T, et al. (2016) Stable isotope dietary reconstructions of herbivore enamel reveal heterogeneous wooded savanna ecosystems in the Plio-Pleistocene Malawi rift. *Palaeogeogr Palaeoclimatol Palaeoecol* 459:170–181.
- Kohn MJ, Cerling TE (2002) Stable isotope compositions of biological apatite. *Phosphates. Geochemical, Geobiological, and Materials Importance*, Reviews in Mineralogy and Geochemistry, eds Kohn MJ, Rakovan J, Hughes JM (Mineral Soc Am, Washington, DC), Vol 48, pp 455–488.
- Kullmer O (2008) The fossil suidae from the Plio-Pleistocene Chiwondo Beds of northern Malawi, Africa. *J Vertebr Paleontol* 28:208–216.
- Kim S-T, O'Neil JR, Hillaire-Marcel C, Mucci A (2007) Oxygen isotope fractionation between synthetic aragonite and water: Influence of temperature and Mg^{2+} concentration. *Geochim Cosmochim Acta* 71:4704–4715.
- Kim S-T, O'Neil JR (1997) Equilibrium and nonequilibrium oxygen isotope effects in synthetic carbonates. *Geochim Cosmochim Acta* 61:3461–3475.
- Passey BH, Levin NE, Cerling TE, Brown FH, Eiler JM (2010) High-temperature environments of human evolution in East Africa based on bond ordering in paleosol carbonates. *Proc Natl Acad Sci USA* 107:11245–11249.
- Peel MC, Finlayson BL, McMahon TA (2007) Updated world map of the Köppen-Geiger climate classification. *Hydrol Earth Syst Sci* 11:1633–1644.
- Climate-Charts.com (2010) Climate charts. Available at <https://www.climate-charts.com/Locations/m/MW67423.html>. Accessed October 2, 2017.
- Levin NE (2013) *Compilation of East Africa Soil Carbonate Stable Isotope Data*. Available at get.iedadata.org/doi/100231. Accessed February 16, 2018.
- Sponheimer M, de Ruiter D, Lee-Thorp J, Späth A (2005) Sr/Ca and early hominin diets revisited: New data from modern and fossil tooth enamel. *J Hum Evol* 48:147–156.
- Sponheimer M, Lee-Thorp JA (2003) Differential resource utilization by extant great apes and australopithecines: Towards solving the C_4 conundrum. *Comp Biochem Physiol A Mol Integr Physiol* 136:27–34.
- Paine OCC, et al. (2018) Grass leaves as potential hominin dietary resources. *J Hum Evol* 117:44–52.
- Dominy NJ (2012) Hominins living on the sedge. *Proc Natl Acad Sci USA* 109:20171–20172.
- Wynn JG, et al. (2013) Diet of *Australopithecus afarensis* from the Pliocene Hadar Formation, Ethiopia. *Proc Natl Acad Sci USA* 110:10495–10500.
- White TD, et al. (2009) Macrovertebrate paleontology and the Pliocene habitat of *Ardipithecus ramidus*. *Science* 326:87–93.
- Sponheimer M, Lee-Thorp JA (1999) Isotopic evidence for the diet of an early hominid, *Australopithecus africanus*. *Science* 283:368–370.
- van der Merwe NJ, Thackeray JF, Lee-Thorp JA, Luyt J (2003) The carbon isotope ecology and diet of *Australopithecus africanus* at Sterkfontein, South Africa. *J Hum Evol* 44:581–597.
- Lee-Thorp J, et al. (2012) Isotopic evidence for an early shift to C_4 resources by Pliocene hominins in Chad. *Proc Natl Acad Sci USA* 109:20369–20372.
- WoldeGabriel G, et al. (2009) The geological, isotopic, botanical, invertebrate, and lower vertebrate surroundings of *Ardipithecus ramidus*. *Science* 326:65e1–5.
- Spötl C, Vennemann TW (2003) Continuous-flow isotope ratio mass spectrometric analysis of carbonate minerals. *Rapid Commun Mass Spectrom* 17:1004–1006.
- Wacker U, Fiebig J, Schoene BR (2013) Clumped isotope analysis of carbonates: Comparison of two different acid digestion techniques. *Rapid Commun Mass Spectrom* 27:1631–1642.
- Wacker U, et al. (2014) Empirical calibration of the clumped isotope paleothermometer using calcites of various origins. *Geochim Cosmochim Acta* 141:127–144.
- Dennis KJ, Affek HP, Passey BH, Schrag DP, Eiler JM (2011) Defining an absolute reference frame for 'clumped' isotope studies of CO_2 . *Geochim Cosmochim Acta* 75:7117–7131.
- Fiebig J, et al. (2016) Slight pressure imbalances can affect accuracy and precision of dual inlet-based clumped isotope analysis. *Isotopes Environ Health Stud* 52:12–28.
- Uno KT, et al. (2011) Late Miocene to Pliocene carbon isotope record of differential diet change among East African herbivores. *Proc Natl Acad Sci USA* 108:6509–6514.
- Cerling TE, Harris JM, Leakey MG (2003) Isotope paleoecology of the Nawata and Nachukui formations at Lothagam, Turkana Basin, Kenya. *Lothagam: The Dawn of Humanity in Eastern Africa*, eds Leakey MG, Harris JM (Columbia Univ Press, New York), pp 583–604.
- Semaw S, et al. (2005) Early Pliocene hominids from Gona, Ethiopia. *Nature* 433:301–305.
- Harris JM, Cerling TE (2002) Dietary adaptations of extant and Neogene African suids. *J Zool* 256:45–54.
- Bibi F, Souron A, Bocherens H, Uno K, Boisserie J-R (2012) Ecological change in the lower Omo valley around 2.8 Ma. *Biol Lett* 9:20120890.
- Drapeau MSM, et al. (2014) The Omo Mursi formation: A window into the East African Pliocene. *J Hum Evol* 75:64–79.
- Morgan ME, Kingston JD, Marino BD (1994) Carbon isotopic evidence for the emergence of C_4 plants in the Neogene from Pakistan and Kenya. *Nature* 367:162–165.
- Kingston JD (2011) Stable isotopic analyses of Laetoli fossil herbivores. *Paleontology and Geology of Laetoli: Human Evolution in Context*, Geology, Geochronology, Vertebrate Paleobiology and Paleoanthropology Series, ed Harrison T (Springer, Berlin), Vol 1, pp 293–328.